Journal of Electronic Materials (2022) 51:2062–2069
https://doi.org/10.1007/s11664-022-09468-z

ORIGINAL RESEARCH ARTICLE

Investigation of pH Effect on the Performance of Undoped Silicon Carbide Nanowire Field-Effect Transistors for the Development of Chemical Sensors and Biosensors

Habeeb Mousa[1] · **Muhammad Awais**[1] · **Kasif Teker**[1]

Received: 22 June 2021 / Accepted: 21 January 2022 / Published online: 11 February 2022

Abstract
The effect of pH on the performance of undoped silicon carbide nanowire field-effect transistors (SiCNW-FETs) was systematically studied using various solutions with pH ranging from pH 2 to pH 13 and important transport parameters such as transconductance, mobility, and resistivity were reported. Interestingly, at 2 V, alkaline solutions with high pH value (pH 13) revealed a higher transconductance of 7.13 nS and lower resistivity of 40 Ω cm as compared to acidic solutions with 0.01 nS and $2.1x10^4$ Ω cm at pH 2, respectively. A model describing the pH-dependent conductance of the SiCNW-FETs was proposed. Moreover, a comprehensive comparison of the pH effects on the transport properties of the undoped SiCNW-FETs and nitrogen-doped SiCNW-FET was presented and the measurements clearly revealed opposite trends for a wide range of pH solutions. In short, our SiCNW-FETs with high sensitivity, high stability, and minuscule sample volume can provide solutions for the development of harsh environment compatible nanosensors for chemical, biochemical, and environmental sensing applications.

Keywords pH effect · biochemical sensing · undoped SiC nanowires · SiCNW-FETs · environmental sensing

Introduction

Nanostructured materials have been extensively studied for the past two decades due to their interesting and unique thermal, electronic, mechanical, and optical properties.[1–3] Nanostructured materials with their high surface-to-volume ratio, single crystallinity, and high sensitivity have led to an explosion of utilization of these materials in a variety of sensing applications such as medical, biochemical, and food inspection.[4–6] In recent years, a tremendous amount of progress has been made in the field of one-dimensional semiconductor nanostructures. Among the various classes of one-dimensional nanomaterials, semiconductor nanowires offer good building blocks for the fabrication of various devices on nanoscale due to their ability to be integrated into electronic devices, their large tolerance for mechanical deformation, and their capability of doping modulation.[7]

The technological interest in wide band gap (WBG) semiconductors such as silicon carbide (SiC), gallium nitride (GaN), zinc oxide (ZnO), and aluminum nitride (AlN) has sensibly increased through the years because of their applications in optoelectronics and high-power electronic devices.[8,9] Among the WBG semiconductors, SiC has been recognized as an important material with a wide range of industrial applications. It possesses excellent properties such as good physical stability at harsh conditions, high thermal conductivity, high electron mobility, and high breakdown voltage characteristics.[10,11] These advantages make it a great material for the fabrication of electronic and sensing devices operating in high-temperature, high-power, high-frequency, and harsh environments.[12] Thus, capability to perform in harsh conditions make SiC an attractive candidate for pH sensors to be used in a wide range of applications such as monitoring of environmental and chemical processes, manufacturing, processing of food, and supporting basic research.[2,13,14] Until now, only a few groups have studied the effect of pH on semiconductor materials. For instance, the fabrication and characterization of undoped polysilicon nanowire as a pH sensor was reported.[2] The work demonstrated that variation in pH from pH 2 to pH 12 results

✉ Kasif Teker
kteker@hotmail.com; kasif.teker@marmara.edu.tr

[1] Faculty of Engineering, Advanced Micro- and Nano-Devices Laboratory, Marmara University, Istanbul, Turkey

in the reduction of current by 1.2 times due to the higher concentration of OH^- and deprotonation of SiOH groups. Similar work was done by the same group of researchers on doped polysilicon nanowire as a biosensor showing opposite trends in current of the undoped nanowire for the same ranges of pH. The conductivity of the polysilicon nanowire was influenced by the majority of positive surface charges.[15] Furthermore, fabrication and characterization of the AlN gate ion-sensitive field-effect transistor (ISFET) pH sensor was reported.[16] It was found that the sensitivity of ISFET was significantly affected by primary amine site density and dissociation constant for AlN sensing film.[16] Very recently, we have reported the effect of pH on transport characteristics of nitrogen-doped silicon carbide nanowire field-effect transistors. The device showed a high transconductance (4.5 mS) and very low resistivity (0.065 mΩ cm) at pH 5 at a low voltage of 2 V.[17] Nevertheless, there exists great room for improvement and new studies involving semiconductor nanowire devices for pH sensing applications.

In this work, we report an investigation of the effect of pH on the performance of undoped SiCNW-FET devices by applying various pH solutions from pH 2 to pH 13. Important electrical properties including transconductance, mobility, resistivity, and stability of the SiCNW-FETs were investigated. The device showed a high transconductance of 7.13 nS and low resistivity of 40 Ω cm for an alkaline solution (pH 13) at 2 V. However, the device demonstrated lower transconductance of 0.01 nS and higher resistivity of 2.1×10^4 Ω cm in an acidic solution (pH 2) at 2 V. SiCNW-FETs exhibited very good and distinct responses to the pH changes offering new insights for future device technologies for chemical and biosensing applications.

Experimental Details

The fabrication of the SiCNW-FETs took place through a "bottom-up" fabrication approach. The bottom-up approach enables simple and low-cost fabrication of the devices due to a fewer number of fabrication steps compared to the top-down approach. The fabrication process started with the growth of silicon carbide nanowires (SiCNWs) in a horizontal cold-wall RF-induction heated metal organic chemical vapor deposition (MOCVD) reactor at atmospheric pressure. The process was followed by the alignment of the SiCNWs through the dielectrophoresis (DEP) assembly method. The DEP assembly of nanowires has been very attractive due to the ability to position nanowires precisely on any substrate. The DEP method eliminates some constraints imposed by thermal and chemical incompatibilities between substrate and nanowires. The highly anisotropic morphology of nanowires and large spontaneous polarization enables the alignment of these nanowires into NWFET devices. Thus, it is a low-cost, precise, rapid, and convenient device fabrication approach. To go deeper into the growth process, a highly doped SiO_2 /Si substrate was cleaned by using the standard cleaning procedure of acetone and isopropyl alcohol (IPA) for 2 min. Finally, the wafer was rinsed with deionized (DI) water and dried with nitrogen before placing it on a graphite susceptor. The synthesis of the SiCNWs was catalytically assisted by nickel (Ni) nanoparticles. The system was prepared for the growth of SiCNWs by heating it to 1100°C concurrently with a flow of argon (Ar, 99.9999%) and hydrogen (H_2, 99.999%) at rates of 500 standard cubic centimeters per minute (sccm), and 100 sccm, respectively. Then, the growth process was initiated by introducing 10 sccm of hexamethyldisilane (HMDS) (purity > 98%, Gelest, Inc.), 200 sccm of H_2, and 500 sccm of Ar for a time period of 15 min. Subsequently, the synthesized SiCNWs were suspended in IPA solution and then sonicated for approximately 13 h to separate the tangled nanowires to be used in device fabrication. The morphology of the synthesized nanowires was analyzed using scanning electron microscopy (SEM, Phenom XL). Additionally, the chemical bond structure of the as-grown nanowires was characterized by Fourier transform infrared spectroscopy (FTIR) (FTS 7000 Series DigiLab with a UMA 600 microscope).

Next, the SiCNW-FETs were fabricated over pre-patterned electrodes (Ti/Au = 10/90 nm) on a heavily doped p-type Si substrate with SiO_2 as an insulator layer using DEP assembly. Two devices were fabricated: device "A" with two nanowires and device "B" with three nanowires. To start with, a 0.1-µl drop from the suspended nanowire solution was taken and placed on the selected gap (channel width of 2.5 µm) between the electrodes using a micropipette. Subsequently, AC peak-to-peak voltage (V_{pp}) of 5 V, sine wave, and a frequency of 20 kHz were applied through a function generator. The same procedure was used in the fabrication of both devices (A and B).

The pH solutions ranging from pH 2 to pH 13 were prepared by titrating DI water into solutions of dilute hydrochloric acid (HCl, 37.0%) and potassium hydroxide (KOH, ≥ 85.0%). The pH of each solution was monitored by a pH meter. A drop (~ 0.5 µl) of each pH solution was applied on the gap using a micropipette and was allowed to dry for about 8 min at room temperature. Then, the device was dipped into DI water to remove any residue before taking the measurements. The electrical responses of the devices to the pH solutions were recorded using a Keithley 2634B source meter and the data were collected using Labview.

Results and Discussion

The growth of the SiCNWs on SiO_2/Si substrate with Ni as a catalyst was accomplished through a single-step growth at 1100°C for 15 min. After the growth of the SiC nanowires,

surface morphology and dimensional analyses of the nanowires were conducted by SEM as depicted in Fig. 1a. Based on the SEM image, high-density grown nanowires with diameters ranging from 20 to 90 nm and an average length of 20 µm were determined. Following the morphological studies, FTIR measurements were conducted to determine chemical bond states of the SiC nanowires. Figure 1b shows the FTIR spectrum of the SiC nanowires grown on SiO_2/Si substrate. The spectrum shows a strong SiC transverse optical (TO) absorption at 793 cm^{-1} and the broad longitudinal optical (LO) absorption around 950 cm^{-1}. It is worth noting that the sharp and high intensity Si-C absorption peak (TO) indicates good bonding uniformity of the SiC nanowires. Following characterization studies, the SiCNW devices have been fabricated through the dielectrophoresis method (DEP), which can be considered as an effective self-assembly technique to align and position nanowires in selected areas by applying a certain frequency and electric field to the electrodes. Figure 1c shows a SEM image of device "A" after the nanowire alignment between the Au electrodes. The figure reveals that the two nanowires are well-aligned between the two Au electrodes. In order to improve the conformity between the contacts and the SiC nanowires, the devices were annealed at 300°C for 5 min.[18] In order to portray the fabrication of the devices clearly, Fig. 2 shows the experimental flow chart of the sample preparation and measurement setup with the device schematic.

After finishing the fabrication process, the electrical characteristics of both devices "A" and "B" were investigated subsequently at different pH solutions. Important figures of

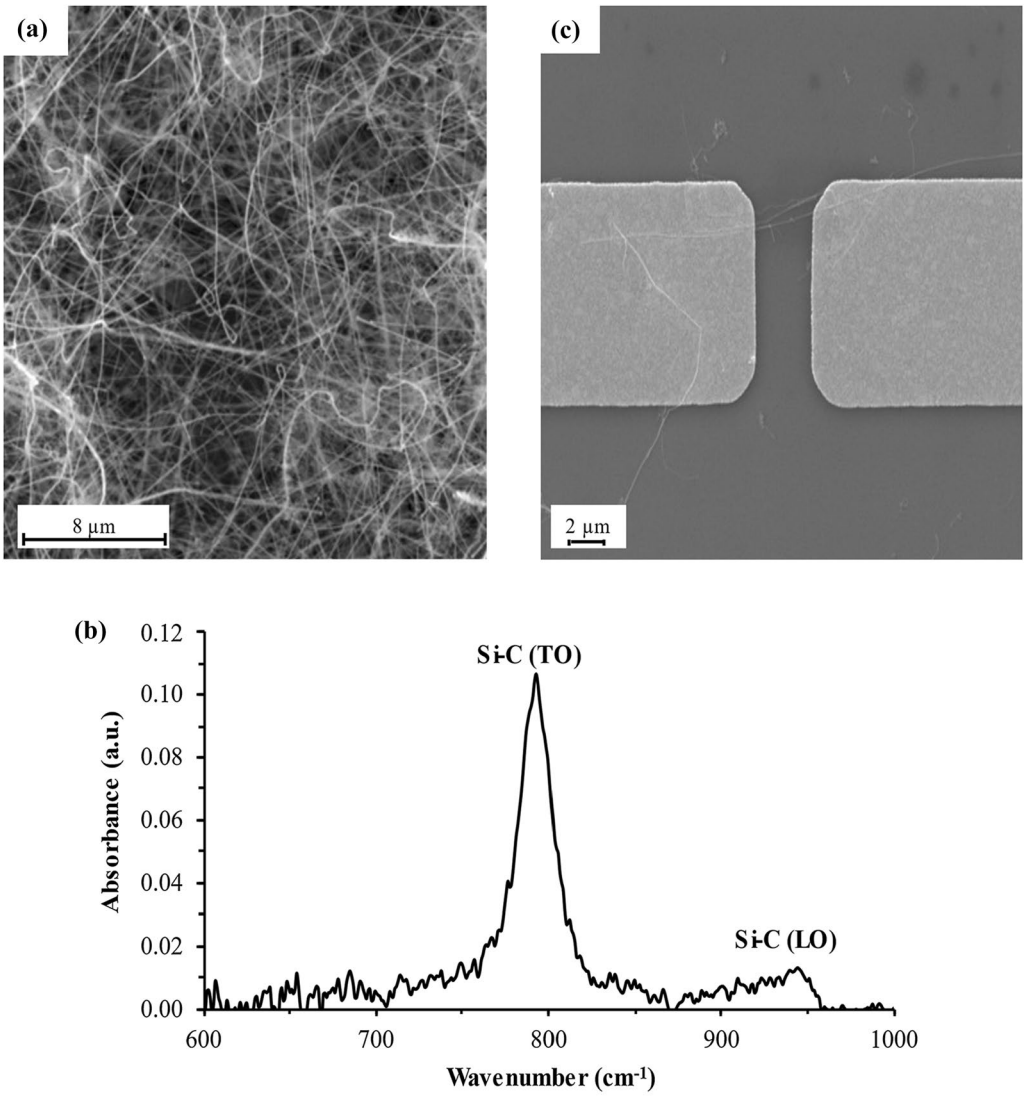

Fig. 1 (a) SEM image of the grown 3C-SiC nanowires on SiO_2/Si substrate (scale bar of 8 µm); (b) FTIR spectrum of the SiC nanowires showing a strong absorption peak at ~ 793 cm^{-1} associated to the SiC transverse optical (TO) absorption; (c) SEM image of the fabricated SiCNW-FET consisting of two nanowires (scale bar of 2 µm).

merit including transconductance (gm), mobility (μ), and resistivity (ρ) were computed in order to evaluate the devices sensing performance. A three-terminal configuration was considered. The two Au electrodes act as drain and source, while the highly doped p-type Si acts as a back gate and is responsible for modulating the channel conductance. To start with, the current (I_{ds}) versus voltage (V_{ds}) curves of device "A" were acquired at different pH values starting from pH 13 and followed by pH 11, 7, 5, 3, and 2. The measurements were conducted by sweeping the voltage from − 2 to 2 V with a step voltage of 0.2 V. The gate voltage (V_g) was kept at 0 V throughout the measurements. Figure 3a demonstrates a typical I_{ds} versus V_{ds} curves of device "A" after applying pH solutions. From the results obtained, pH 13 is at the top with the highest current of 6.38 nA at 2 V. As the pH value of the injected solution was decreased from pH 13 to pH 2, the drain current was reduced from 6.38 nA (pH 13) to 2.68 nA (pH 7) and finally reached 0.019 nA at pH 2. In order to determine the transport properties of the SiCNW-FETs, I_{ds} versus V_g measurements were conducted by sweeping gate voltage from − 2 to 2 V with constant V_{ds} of 0.01 V. Figure 3b shows the recorded $I_{ds} - V_g$ curves of device "A" after applying various solutions with pH ranging from 2 to 13. Similar trends with the $I_{ds} - V_{ds}$ curves were observed with pH 13 with highest and pH 2 with the lowest current values. A high current of 8.4 nA was recorded for pH 13, then the current was reduced to one fourth that after applying pH 7 solution. When the pH was further reduced from pH 7 to 2, the current decreased from 2.12 nA to 0.01 nA, respectively. Furthermore, $I_{ds} - V_g$ exhibits a strong decrease in drain-source current as the gate voltage changes from − 2 V to 0 V indicating that the nanowires have p-type conductance (unintentional).[19]

The observed changes in conductance of the SiCNW-FET after the application of different pH solutions can be explained as follows: According to the oxide/electrolyte interface model,[4] when SiC is hydrolyzed by an aqueous solution such as diluted HCl or diluted KOH, the chemical reaction will result in SiO_2 as a product. Furthermore, when SiO_2 is subjected to an aqueous solution with a specific pH, the material gets hydrolyzed into ionizable sites and results in producing potential determining ions H^+ or OH^-. These available sites have the capability to either accept hydrogen ions by adsorption mechanism or release them in a dynamic exchange process according to the description of the binding site model.[20] The pH response is determined

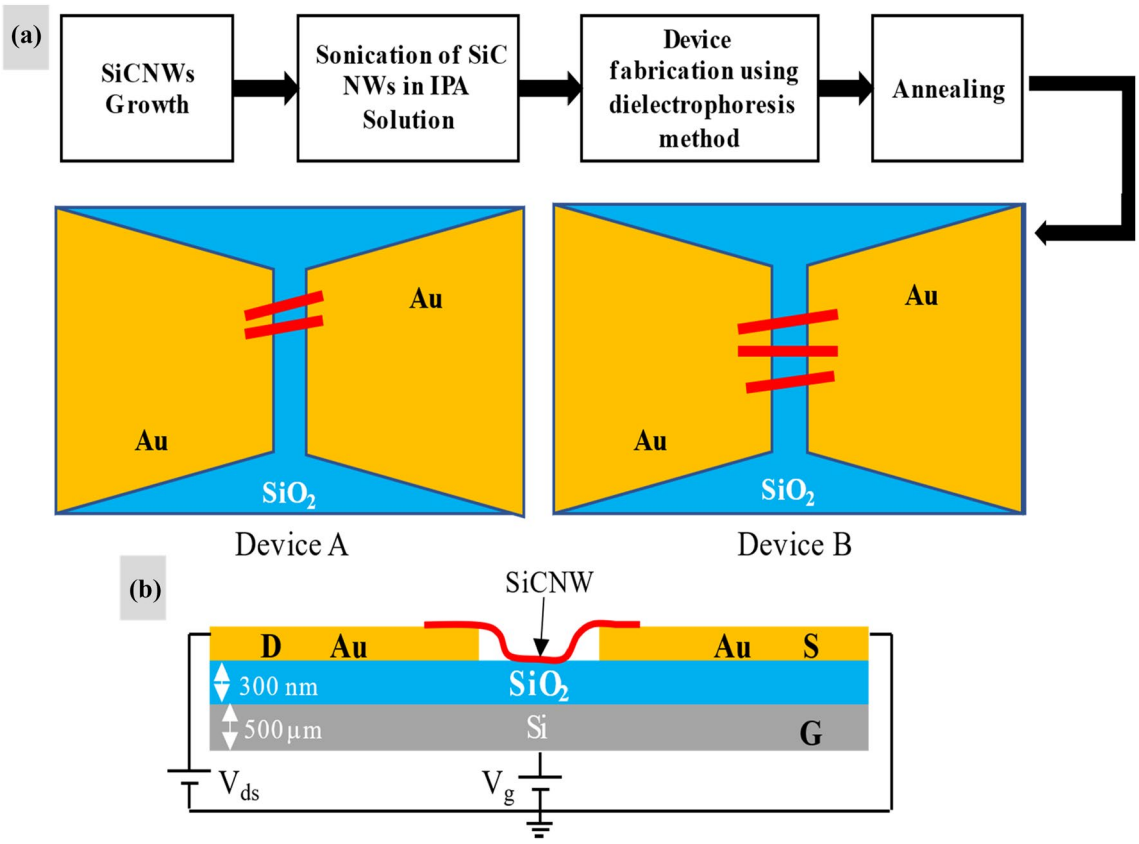

Fig. 2 (a) Experimental flow chart of the sample preparation as well as top views of devices "A" and "B"; (b) Schematic diagram of the experimental setup used to investigate the effect of pH on the performance of SiCNW-FETs.

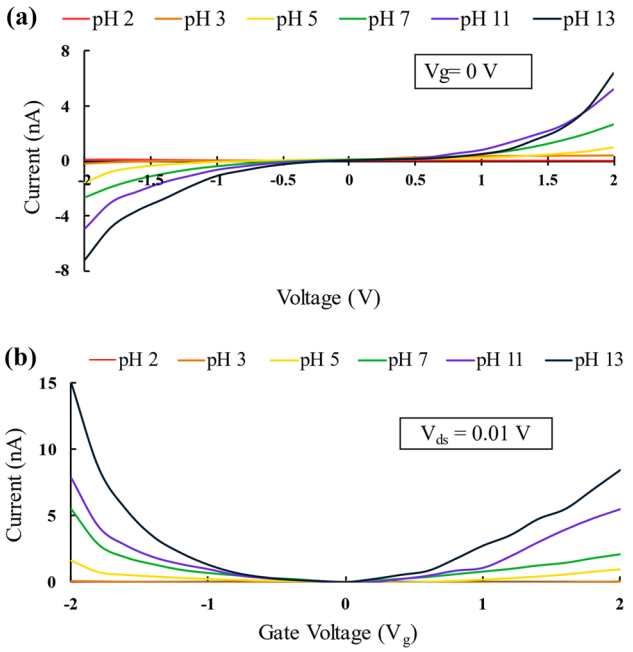

Fig. 3 (a) Current (I_{ds}) versus drain- source voltage (V_{ds}) curves of device "A" (two SiCNWs) with constant gate voltage (V_g) of 0 V after applying different pH values (pH 2, pH 3, pH 5, pH 7, pH 9, pH 11, and pH 13); (b) $I_{ds} - V_g$ curves of device "A" while keeping V_{ds} constant (0.01 V) at various pH values ranging from pH 2 to pH 13.

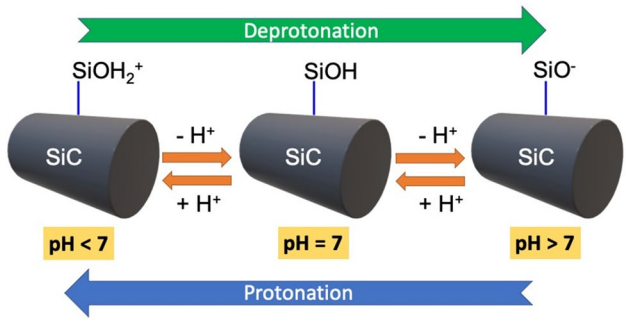

Fig. 4 A model illustrating the pH-dependent surface charges due to the interaction of the surface silanol (SiOH) group with the hydrogen ions (H^+) through protonation and deprotonation mechanisms.

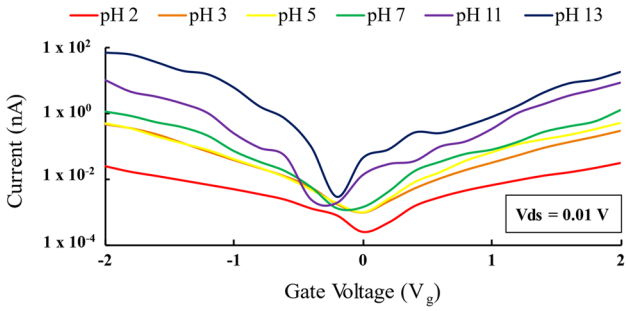

Fig. 5 Current (I_{ds}) versus gate voltage (V_g) curves of device "B" after the application of different solutions with pH values ranging from pH 2 to pH 13. The device demonstrated similar trend as device "A", in which pH 13 has the largest current and pH 2 has the lowest current.

by the interaction of the surface silanol (SiOH) group produced from the hydrolysis of SiO_2[2,21] with the H^+ ions. This interaction can be briefly explained by two main processes, namely protonation (addition of cations) and deprotonation (removal of cations). In alkaline solutions (pH > 7), SiOH gets deprotonated to SiO^- ions due to the higher concentration of OH^-. At pH 13, this process generates more negative ions, which anchor to the surface of the SiCNWs. This causes less hole carrier depletion to occur and correspondingly increases the conductance of the device. Conversely, for acidic solutions (pH < 7) there is a higher proportion of H^+ ions which leads to the protonation of SiOH and results in $SiOH_2^+$ ions. The concentration of $SiOH_2^+$ ions released by the protonation of SiOH depends on the pH of the solution. The more acidic the solution is, the more positive ions will be adsorbed to the surface of the SiC nanowires, and thus the surface becomes depleted of charge carriers (holes). As a result, the resistance of the device increases and the device conductance decreases. In order to simplify the mechanism behind the changes in conductance after applying the different pH solutions, a model illustrating the interaction of the surface silanol (SiOH) group with the hydrogen ions (H^+) is presented in Fig. 4. The resulting pH-dependent electrical surface charge density of the SiC nanowire leads to a modulation in the device conductance, and hence the drain current of the transistor.

In order to provide further verification of our results, the same experimental procedure was repeated for device "B" under the same conditions. Figure 5 shows the acquired $I_{ds} - V_g$ curves of the device after applying pH solutions with pH values ranging from pH 2 to pH 13. The measurements were taken by sweeping the voltage from − 2 V to 2 V at a constant V_{ds} of 0.01 V. The figure shows that the highest current of 17.36 nA was observed at pH 13 at a gate voltage of 2 V. Furthermore, a change in pH from pH 13 to 2 results in a decrease of current from 17.36 nA to 0.03 nA at 2 V. Device "B" demonstrated a similar tendency as observed in device "A". The higher current values of device "B" are due to a higher number of nanowires at the channel compared to device "A".

For further analysis of our device, transconductance (gm), which is an important parameter in evaluating the speed of a transistor in switching between on and off states was calculated. Figure 6 shows the plots of the transconductance versus pH for both devices "A" and "B". *gm* was extracted from the $I_{ds} - V_g$ curves by taking the slope ($\partial I_{ds}/\partial V_g$) between 0.6 V to 1.6 V. For device "A", it starts off with a value of 5.56 pS for pH 2 and a significant increase to 4.7 nS at pH

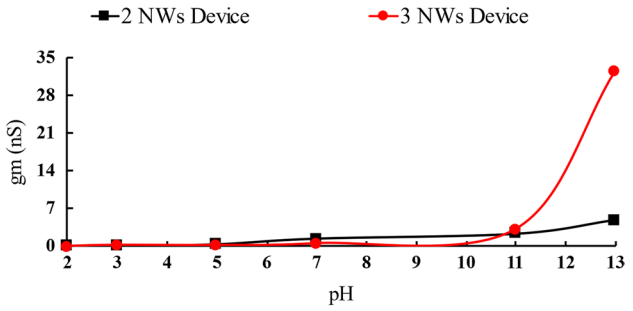

Fig. 6 The transconductance (gm) of the SiCNW-FET devices at various pH solutions.

13. Similarly, the transconductance values for device "B" were calculated as 13 pS for pH 2 and 7.13 nS for pH 13 showing a substantial improvement in transconductance in alkaline solutions. In comparing our device to a recent work on poly-Silicon nanowire sensors similar transconductance values have been reported with ~75 pS and ~ 600 pS at pH 3 and pH 12, respectively.[22] The significant variation in transconductance at various pH solutions can be attributed to the changes in surface charge density of the nanowire as proposed in the aforementioned model. In an attempt to further discuss the transport properties of the SiCNW-FET devices at various pH solutions, we computed the corresponding carrier mobilities (μ). The carrier mobility (μ) can be calculated by the equation, $\mu = g_m L^2/(CV_{ds})$, where L is the channel length, and C is the capacitance of the nanowire (1.97×10^{-16} F). The capacitance of the nanowire can be estimated from the cylinder-plate capacitance model by, $C = 2\pi\varepsilon\varepsilon_0 L/\ln(2h/r)$, in which and ε_o are dielectric constants of SiO_2 (3.9) and permittivity of vacuum (8.854×10^{-14} F/cm), h is the thickness of SiO_2 layer (300 nm), and r is the radius of the nanowire. The carrier mobility in device "A" increased from 0.17 $cm^2(V\ s)^{-1}$ to 150 $cm^2(V\ s)^{-1}$ with the increase from pH 2 to pH 13, respectively. The similar trend was observed in device "B", where the mobility increased from 0.430 $cm^2(V\ s)^{-1}$ at pH 2 to 226 $cm^2(V\ s)^{-1}$ at pH 13. The mobility results support the changes in conductance of the SiCNW-FETs in acidic and alkaline solutions.

Next, we have computed the change in resistivity (ρ) at different pH solutions at 2 V. The resistivity can be calculated by, $\rho = (V_{ds} \cdot \pi \cdot r^2)/(I_{ds} \cdot L)$, where V_{ds} is the drain-source voltage, r is the radius of the nanowire, I_{ds} is the drain-source current, L is the channel length of the fabricated device. The calculated resistivity values for device "A" were 3.8×10^4 Ω cm and 1.1×10^2 Ω cm at pH 2 and pH 13, respectively. A similar trend was observed in device "B" with the highest resistivity of 2.1×10^4 Ω cm at pH 2 and the lowest 4.0×10^1 Ω cm at pH 13. In consequence, an acidic solution leads to an increase in resistivity, whereas a basic solution leads to a decrease in resistivity supporting our proposed model.

Last but not least, it is worth comparing the pH effects on the undoped SiCNW-FET and our recently reported study on nitrogen-doped SiCNW-FET.[17] Interestingly, the nitrogen-doped SiCNW-FET showed an opposite trend compared to the undoped SiCNW-FET. In fact, the nitrogen-doped SiCNW-FET resulted in a high current in acidic environments (pH 5) and a low current for alkaline environments (pH 9), which is likely due to the difference in conductivity type of the SiC nanowires. Table I provides a comprehensive comparison of the pH effects on the transport properties of the undoped SiCNW-FETs (A and B) and nitrogen-doped SiCNW-FET, clearly revealing opposite trends for a wide range of pH solutions. The opposite trend between the nitrogen-doped SiCNW-FET and the undoped SiCNW-FET can be postulated as follows: For the nitrogen-doped SiCNW-FETs, the more acidic the solution is, the more H^+ ions will be adsorbed to the surface of the doped SiC nanowires, creating a chain of metallic surface states and causing an increase in the surface charge density. Correspondingly, this increases the conductance of the device. However, for the undoped device, in acidic solutions, the H^+ ions will protonate the SiOH into $SiOH^{2+}$. These ions will be adsorbed to the surface of the SiC nanowires, and thus the surface becomes depleted of charge carriers (holes), which will reduce the conductance. In summary, high sensitivity, high stability, and low sampling size make

Conclusions

The effect of pH on the electrical transport properties of the undoped SiCNW-FET devices have been successfully demonstrated for a broad range of pH from 2 to 13. In fact, alkaline solutions with pH 13 resulted in a higher transconductance of 7.13 nS and lower resistivity of 40 Ω cm as compared to acidic solutions with 0.01 nS and $2.1x10^4$ Ω cm at pH 2, respectively, at 2 V. Additionally, a model describing the pH-dependent conductance of the SiCNW-FETs was proposed. Moreover, a comprehensive comparison of the pH effects on the transport properties of the undoped SiCNW-FETs and nitrogen-doped SiCNW-FET was presented and the measurements clearly revealed opposite trends for a wide range of pH solutions. Consequently, our SiCNW-FETs with high sensitivity, high stability, and minuscule sample volume can provide solutions for the development of harsh environment compatible nanosensors for chemical, biochemical, and environmental sensing applications.

Table I Comparison of the pH effects on the transport properties of the undoped SiCNW-FETs (A and B) and nitrogen-doped SiCNW-FET, clearly revealing opposite trends for a wide range of pH solutions.

Material	pH	Transconductance (nS)	Resistivity (Ω cm)	Mobility $cm^2(V\ s)^{-1}$	Number of NWs	References
Undoped SiCNW-FET	2	0.005	3.8×10^4	1.7×10^{-1}	2	This work
	3	0.01	1.9×10^3	4.3×10^{-1}		
	5	0.54	7.0×10^2	1.7×10^1		
	7	1.06	2.7×10^2	3.4×10^1		
	11	3.51	1.4×10^2	1.1×10^2		
	13	4.72	1.1×10^2	1.5×10^2		
Undoped SiCNW-FET	2	0.01	2.1×10^4	4.3×10^{-1}	3	This work
	3	0.11	2.6×10^3	3.7×10^1		
	5	0.19	2.0×10^3	6.2×10^1		
	7	0.34	7.1×10^2	1.09×10^1		
	11	3.20	6.7×10^1	1.02×10^2		
	13	7.13	4.0×10^1	2.26×10^2		
Nitrogen-doped SiCNW-FET	5	4.5×10^6	6.5×10^{-5}	–	2	17
	7	2.6×10^6	7.9×10^{-5}	–		
	9	1.5×10^5	2.6×10^{-3}	–		

SiCNW-FETs are one of the most promising candidates for the development of environmental and biochemical nanosensors

Acknowledgements KT gratefully thanks the Istanbul Development Agency (ISTKA) for providing funding for this research (Grant No: TR10/16/YNY/0102).

Conflict of interest The authors declare that they have no known competing financial interests or personal relationships that could have appeared to influence the work reported in this paper.

References

1. N.P. Dasgupta, J. Sun, C. Liu, S. Brittman, S.C. Andrews, J. Lim, H. Gao, R. Yan, and P. Yang, 25th Anniversary article: semiconductor nanowires-synthesis, characterization, and applications. *Adv. Mater.* 26, 2137 (2014).
2. C.C. Yee, Md. K. Marshad, M. Nuzaihan, M.F.M. Fathil, and U. Hashim, Fabrication and characterization of undoped polysilicon nanowire for pH sensor. *2014 IEEE Int. Conf. Semicond. Electron.* 396, 1520 (2014).
3. J. Feng, X. Li, G. Zhu, and Q.J. Wang, Emerging high-performance SnS/CdS nanoflowers heterojunction for ultrafast photonics. *ACS Appl. Mater. Interfaces.* 12, 43098 (2020).
4. J. Hsu, B. Huang, C. Huang, and H. Chen, Silicon nanowires as pH sensor. *Jpn. J. Appl. Phys.* 44, 2626 (2005).
5. M. Ham, J. Choi, W. Hwang, C. Park, W. Lee, and J. Myoung, Contact characteristics in GaN nanowire devices. *Nanotechnology* 17, 2203 (2006).
6. H. Zeng, G. Zhang, K. Nagashima, T. Takahashi, T. Hosomi, and T. Yanagida, Metal-oxide nanowire molecular sensors and their promises. *Chemosensors.* 9, 1 (2021).
7. T.H. Kim, S.Y. Lee, N.K. Cho, H.K. Seong, H.J. Choi, S.W. Jung, and S.K. Lee, Dielectrophoretic alignment of gallium nitride nanowires (GaN NWs) for use in device applications. *Nanotechnology* 17, 3394 (2006).
8. F. Roccaforte, F.L. Via, V. Raineri, P. Musumeci, L. Calcagno, and G. Condorelli, Highly reproducible ideal SiC Schottky rectifiers: effects of surface preparation and thermal annealing on the Ni/6H-SiC Barrier height. *Appl. Phys. A Mater. Sci. Process.* 77, 827 (2003).
9. K. Teker, Density and morphology adjustments of gallium nitride nanowires. *Appl. Surf. Sci.* 283, 1065 (2013).
10. P. Tanner, A. Iacopi, H. Phan, S. Dimitrijev, L. Hold, K. Chaik, G. Walker, D.V. Dao, and N. Nguyen, Excellent rectifying properties of the N-3C-SiC/p-Si Heterojunction subjected to high Temperature annealing for electronics, MEMS, and led applications. *Sci. Rep.* 7, 10025 (2017).
11. K. Rogdakis, M. Bescond, E. Bano, and K. Zekentes, Theoretical comparison of 3C-SiC and Si nanowire FETs in ballistic regime. *Mater. Sci. Forum* 579, 600 (2008).
12. A. Meng, M. Zhang, J. Zhang, and Z. Li, Synthesis and field emission properties of silicon carbide nanobelts with a median ridge. *CrystEngComm* 14, 6755 (2012).
13. J. Ahn, J. Kim, M. Seol, D.J. Baek, Z. Guo, C. Kim, S. Choi, and Y. Choi, A pH sensor with a double-gate silicon nanowire field-effect transistor. *Appl. Phys. Lett.* 102, 083701 (2013).
14. J. Jang, S. Choi, J. Kim, T.J. Park, B. Park, D.M. Kim, S.J. Choi, S.M. Lee, D.H. Kim, and H. Mo, Effect of liquid gate bias rising time in pH sensors based on Si nanowire ion sensitive field effect transistors. *Solid-State Electron.* 140, 109 (2018).
15. S.C. Stephen, Md. K. Marshad, Md. N. Mnor, M.F.M. Fathil, A.R. Ruslinda, and U. Hashim, Fabrication and characterization of doped polysilicon nanowire for pH sensor. *Appl. Mech. Mater.* 561, 754 (2015).
16. S. Sinha, R. Mukhiya, R. Sharma, P.K. Khanna, and V.K. Khanna, Fabrication, characterization and electrochemical simulation of AlN-gate ISFET pH sensor. *J. Mater. Sci. Mater. Electron.* 30, 7163 (2019).
17. M. Awais, H. Mousa, and K. Teker, Effect of pH on transport characteristics of silicon Carbide Nanowire field-effect transistor (SiCNW-FET). *J. Mater. Sci. Mater. Electron.* 32, 3431 (2021).

18. S. Paiman, T.H. Ling, M. Husham, and S. Sagadevan, Significant effect on annealing temperature and enhancement on structural, optical and electrical properties of zinc oxide nanowires. *Results Phys.* 17, 103185 (2020).
19. A. Uzun, and K. Teker, Silicon carbide nanowire field effect transistors with high on/off current ratio. *Microelectron. Eng.* 205, 59 (2019).
20. D.E. Yates, S. Levine, and T.W. Healy, Site-binding model of the electrical double layer at the oxide/water interface. *J. Chem. Soc. Faraday Trans.* 70, 1807 (1974).
21. S.F.A. Rahman, N.A. Yusof, U. Hashim, and Md. N. Mnor, Design and Fabrication of Silicon Nanowire based Sensor. *Int. J. Electrochem. Sci.* 8, 10946 (2013).
22. S. Tang, J. Yan, J. Zhang, S. Wei, Q. Zhang, J. Li, M. Fang, S. Zhang, E. Xiong, Y. Wang, J. Yang, Z. Zhang, Q. Wei, H. Yin, W. Wang, and H. Tu, Fabrication of low cost and low temperature poly-silicon nanowire sensor arrays for monolithic three-dimensional integrated circuits applications. *Nanomaterials* 10, 2488 (2020).